

This document contains a post-print version of the paper

Dynamical Model of Axially Moving Steel Strips

authored by M. Saxinger, A. Steinböck, M. Baumgart, and A. Kugi

and published in *Proceedings of the 17th IFAC Symposium on Control, Optimization and Automation in Mining, Mineral and Metal Processing (MMM)*.

The content of this post-print version is identical to the published paper but without the publisher's final layout or copy editing. Please, scroll down for the article.

Cite this article as:

M. Saxinger, A. Steinböck, M. Baumgart, and A. Kugi, "Dynamical model of axially moving steel strips", in *Proceedings of the 17th IFAC Symposium on Control, Optimization and Automation in Mining, Mineral and Metal Processing (MMM)*, vol. 49, Vienna, Austria, 31.08.-02.09. 2016, pp. 190–195. DOI: [10.1016/j.ifacol.2016.10.119](https://doi.org/10.1016/j.ifacol.2016.10.119)

BibTeX entry:

```
% This file was created with JabRef 2.9.2.  
% Encoding: Cp1252
```

```
@INPROCEEDINGS{acinpaper,  
  author = {Saxinger, M. and Steinböck, A. and Baumgart, M. and Kugi, A.},  
  title = {Dynamical Model of Axially Moving Steel Strips},  
  booktitle = {Proceedings of the 17th IFAC Symposium on Control, Optimization and  
    Automation in Mining, Mineral and Metal Processing (MMM)},  
  year = {2016},  
  volume = {49},  
  number = {20},  
  pages = {190--195},  
  address = {Vienna, Austria},  
  month = {31.08.-02.09.},  
  doi = {10.1016/j.ifacol.2016.10.119},  
  issn = {2405-8963}  
}
```

Link to original paper:

<http://dx.doi.org/10.1016/j.ifacol.2016.10.119>

Read more ACIN papers or get this document:

<http://www.acin.tuwien.ac.at/literature>

Contact:

Automation and Control Institute (ACIN)
Vienna University of Technology
Gusshausstrasse 27-29/E376
1040 Vienna, Austria

Internet: www.acin.tuwien.ac.at
E-mail: office@acin.tuwien.ac.at
Phone: +43 1 58801 37601
Fax: +43 1 58801 37699

Copyright notice:

This is the authors' version of a work that was accepted for publication in *Proceedings of the 17th IFAC Symposium on Control, Optimization and Automation in Mining, Mineral and Metal Processing (MMM)*. Changes resulting from the publishing process, such as peer review, editing, corrections, structural formatting, and other quality control mechanisms may not be reflected in this document. Changes may have been made to this work since it was submitted for publication. A definitive version was subsequently published in M. Saxinger, A. Steinböck, M. Baumgart, and A. Kugi, "Dynamical model of axially moving steel strips", in *Proceedings of the 17th IFAC Symposium on Control, Optimization and Automation in Mining, Mineral and Metal Processing (MMM)*, vol. 49, Vienna, Austria, 31.08.-02.09. 2016, pp. 190–195. DOI: [10.1016/j.ifacol.2016.10.119](https://doi.org/10.1016/j.ifacol.2016.10.119)

Dynamical Model of Axially Moving Steel Strips[★]

M. Saxinger^{*} A. Steinboeck^{**} M. Baumgart^{*} A. Kugi^{*}

^{*} *Christian Doppler Laboratory for Model-Based Process Control in the Steel Industry, Automation and Control Institute, Vienna University of Technology, Austria, (e-mail: {saxinger, baumgart, kugi}@acin.tuwien.ac.at).*

^{**} *Automation and Control Institute, Vienna University of Technology, Austria (e-mail: steinboeck@acin.tuwien.ac.at)*

Abstract: Axially moving strips are frequently encountered in industry for various applications. On the one hand, accurate models of transverse displacements of strips are desired for plant design and safety or reliability reasons. On the other hand, the models may serve as a basis for model-based controller and observer design. For the latter also, the complexity of the models should be as low as possible. This work focuses on the development of dynamical models of the motion and elastic deformation of axially moving steel strips guided by rolls. For spatial discretization of both in-plane and out-of-plane motion, the Galerkin weighted residual method is employed and the longitudinal direction of the strip is divided into finite elements. A tailored time integration method is implemented and dynamic simulations for different boundary conditions of a strip in a hot dip galvanizing line are carried out and analyzed. The influence of the geometrical nonlinearity on the transversal displacements of the strip is investigated by means of a faulty air cooler. Finally, the affect of the geometrical nonlinearity on the dynamic and static behavior of the steel strip is investigated in more detail.

Keywords: Mechanical system, Wave equations, Dynamical models, Distributed-parameter system, Mathematical model, Control applications, Steel industry, Numerical simulation.

1. INTRODUCTION

Axially moving flat structures (strips) are typically encountered in many engineering applications. For instance, strip processing in the steel industry, paper production, and foil manufacturing. In such production facilities, strip vibrations can influence the stability of the production process. Moreover, strip vibrations can deteriorate the quality of the processed products. Sophisticated dynamical models are capable of describing the strip vibrations accurately. Another important issue is residual stresses in strips. Residual stresses may occur after thermal treatment or plastic deformation of strips in previous sections of the plant. This results in a curved strip, i.e., crossbow or a coil-set. Hira et al. (1988) addressed this problem for various hot dip galvanizing lines. The residual stresses must be considered in order to achieve accurate models. The dynamical models of axially moving strips are the basis of controller and actuator design, e.g., vibration damping in steel strips or modification of the transversal strip profiles. In order to keep the computing time low, low-dimensional and linear models are desired. In this paper, a dynamical model of axially moving steel strips is derived to investigate the necessity of geometrically nonlinear models for different boundary conditions. Shin et al. (2006) presented a model for dynamic responses of an axially moving mem-

brane without consideration of the bending stiffness and residual stresses. Also, the coupling between in-plane and out-of-plane motion was neglected. This decoupling yields a linear problem, which was solved with the Generalized- α Method. It was presented by Chung and Hulbert (1993) for solving linear problems in the field of structural dynamics. Shearer and Cesnik (2006) proposed an implicit time integration scheme that extends the Generalized- α Method to nonlinear systems. The so called Modified Generalized- α Method will be applied for the nonlinear problems presented in this paper. The spatially discretized model of an axially moving steel strip will serve as basis for the discussion whether the geometrical nonlinearity of the model can be neglected or not.

2. MODELING

2.1 Equations of Motion

A strip element with the displacements \check{u} , \check{v} , and \check{w} along the directions x , y , and z , respectively, is considered. The strip has a uniform thickness h and a mass density ρ . The axial bulk velocity V of the strip is assumed to be constant, g represents the gravitational acceleration, and $q = q(x, y, t)$ is a transversal load. Utilizing the assumptions of the Kirchhoff-Love plate theory, $w(x, y, t)$, $u(x, y, t)$, and $v(x, y, t)$ represent the displacements of a point on the mid-plane of the strip and the displacement \check{w} is independent of z (cf. Reddy, 2007). In the following, the equations of motion for a strip with the boundary

^{*} Financial support by the Austrian Federal Ministry of Science, Research and Economy and the National Foundation for Research, Technology and Development, and voestalpine Stahl GmbH is gratefully acknowledged.

conditions in Fig. 1 will be derived. Hamilton's principle for open systems states that

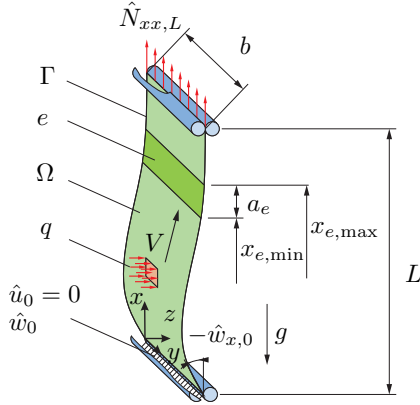


Fig. 1. Plate model in a section between four rolls (boundary condition A).

$$0 = \int_{t_0}^{t_1} (\delta U + \delta G - \delta K + \delta W + \delta M) dt \quad (1)$$

holds, where U is the strain energy, G is the potential energy due to gravity, K is the kinetic energy, W is the work done by applied forces, M is the momentum transport through the boundaries, and t_0 and t_1 are arbitrary points in time. The variation of the strain energy can be written in the form

$$\delta U = \int_{\Omega} (N_{xx} \delta \epsilon_{xx}^0 + M_{xx} \delta \epsilon_{xx}^1 + N_{yy} \delta \epsilon_{yy}^0 + M_{yy} \delta \epsilon_{yy}^1 + N_{xy} \delta \gamma_{xy}^0 + M_{xy} \delta \gamma_{xy}^1) dx dy, \quad (2)$$

where

$$\begin{bmatrix} \epsilon_{xx}^1 \\ \epsilon_{yy}^1 \\ \gamma_{xy}^1 \end{bmatrix} = \begin{bmatrix} -\partial_x^2 w \\ -\partial_y^2 w \\ -2\partial_x \partial_y w \end{bmatrix}, \quad \begin{bmatrix} \epsilon_{xx}^0 \\ \epsilon_{yy}^0 \\ \gamma_{xy}^0 \end{bmatrix} = \begin{bmatrix} \partial_x u + \frac{1}{2}(\partial_x w)^2 \\ \partial_y v + \frac{1}{2}(\partial_y w)^2 \\ \partial_y u + \partial_x v + \partial_x w \partial_y w \end{bmatrix} \quad (3)$$

are curvatures and membrane strains, respectively. The stress resultants N_{xx} , N_{yy} , and N_{xy} are forces per unit width and M_{xx} , M_{yy} , and M_{xy} are moments per unit width. The variation of the potential energy due to gravity reads as

$$\delta G = \rho g h \int_{\Omega} \delta u dx dy, \quad (4)$$

the variation of the kinetic energy can be expressed as

$$\delta K = \rho \int_{\Omega} \int_{-\frac{b}{2}}^{\frac{b}{2}} \mathbf{v}^T \delta \mathbf{v} dz dx dy, \quad (5)$$

with the total velocity vector

$$\mathbf{v} = [V + \partial_t u + V \partial_x u, \quad \partial_t v + V \partial_x v, \quad \partial_t w + V \partial_x w]^T,$$

which results from the material derivative. The virtual work done by a distributed transversal load $q(x, y, t)$ as well as the virtual work caused by the tensile load $\hat{N}_{xx,L}$ take the form

$$\delta W = - \int_{\Omega} q \delta w dx dy - \int_0^b \hat{N}_{xx,L} \delta u|_{x=L} dy. \quad (6)$$

With the variation of the displacement vector

$$\delta \mathbf{r} = [\delta u, \quad \delta v, \quad \delta w]^T,$$

the variation of the momentum transport (cf. McIver, 1973) follows as

$$\delta M = \rho V \int_0^b \int_{-\frac{b}{2}}^{\frac{b}{2}} (\mathbf{v}^T \delta \mathbf{r})|_{x=0}^{x=L} dz dy. \quad (7)$$

Insertion of (2), (4), (5), (6), and (7) into (1) yields the dynamic equations of the strip. Supposing quasi-static relations for the in-plane displacements u and v , the equations of motion read as

$$\mathcal{D}_u = \rho h (V^2 \partial_x^2 u + g) - \partial_x N_{xx} - \partial_y N_{xy} = 0 \quad (8a)$$

$$\mathcal{D}_v = \rho h V^2 \partial_x^2 v - \partial_y N_{yy} - \partial_x N_{xy} = 0 \quad (8b)$$

$$\begin{aligned} \mathcal{D}_w = \rho h (V^2 \partial_x^2 w + 2V \partial_x \partial_t w + \partial_t^2 w) \\ - \partial_x^2 M_{xx} - 2\partial_x \partial_y M_{xy} - \partial_y^2 M_{yy} - q \\ - \partial_x (N_{xx} \partial_x w + N_{xy} \partial_y w) \\ - \partial_y (N_{xy} \partial_x w + N_{yy} \partial_y w) = 0, \end{aligned} \quad (8c)$$

where suitable boundary conditions can be found in Section 2.3. The initial conditions are given by

$$w(x, y, 0) = w_0 \quad \text{and} \quad \partial_t w(x, y, 0) = w_1. \quad (9)$$

2.2 Material Model

The terms N_{xx} , N_{yy} , and N_{xy} couple the differential equations (8). For the simpler case of an axially moving rod, this coupling effect was analyzed in (Steinböck et al., 2015). Based on the findings published there, it can be argued that the assumptions $\partial_t u \approx 0$ and $\partial_t v \approx 0$ are tenable. Using Hooke's law and considering residual stresses from prior deformation, the stress resultants follow in the form

$$\begin{bmatrix} M_{xx} \\ M_{yy} \\ M_{xy} \end{bmatrix} = \frac{Eh^3}{12(1-\nu^2)} \begin{bmatrix} 1 & \nu & 0 \\ \nu & 1 & 0 \\ 0 & 0 & \frac{1-\nu}{2} \end{bmatrix} \begin{bmatrix} \epsilon_{xx}^1 - \epsilon_{xx,res}^1 \\ \epsilon_{yy}^1 - \epsilon_{yy,res}^1 \\ \gamma_{xy}^1 - \gamma_{xy,res}^1 \end{bmatrix}$$

$$\begin{bmatrix} N_{xx} \\ N_{yy} \\ N_{xy} \end{bmatrix} = \frac{Eh}{1-\nu^2} \begin{bmatrix} 1 & \nu & 0 \\ \nu & 1 & 0 \\ 0 & 0 & \frac{1-\nu}{2} \end{bmatrix} \begin{bmatrix} \epsilon_{xx}^0 - \epsilon_{xx,res}^0 \\ \epsilon_{yy}^0 - \epsilon_{yy,res}^0 \\ \gamma_{xy}^0 - \gamma_{xy,res}^0 \end{bmatrix},$$

where E is the Young's modulus and ν is the Poisson's ratio. Six constant residual strain parameters $\epsilon_{xx,res}^1$, $\epsilon_{yy,res}^1$, $\gamma_{xy,res}^1$, $\epsilon_{xx,res}^0$, $\epsilon_{yy,res}^0$, and $\gamma_{xy,res}^0$ account for prior deformations of the strip. In case of a geometrically linear analysis, the higher order terms in (3) are omitted and (8a) and (8b) are independent of (8c).

2.3 Boundary Conditions

A strip with the following boundary conditions is considered: At the bottom boundary ($x = 0$), the displacements $u|_{x=0} = \hat{u}_0 = 0$ and $w|_{x=0} = \hat{w}_0$ and the slope $\partial_x w|_{x=0} = \hat{w}_{x,0}$ are constant. At the upper boundary ($x = L$), the strip is simply supported ($M_{xx}|_{x=L} = 0$, $w|_{x=L} = 0$). In longitudinal direction, two different types of boundary conditions are employed at the upper edge: Boundary condition A is a constant tensile load $N_{xx}|_{x=L} = \hat{N}_{xx,L}$, which is shown in Fig. 1. The geometrical boundary condition B is a constant displacement \hat{u}_L . It relates to the steady-state displacement at the upper roll ($x = L$), which is caused by a tensile load $\hat{N}_{xx,L}$ without any transversal load q acting on the strip. The quantity \hat{u}_L is the averaged displacement value over the width. The remaining lateral boundaries of the strip constitute free edges.

3. DISCRETIZATION AND TIME INTEGRATION

3.1 Spatial Discretization

In order to solve (8) with the associated boundary conditions, the Galerkin weighted residual method is applied. The weak form of the equations of motion follows as

$$\begin{aligned} & \int_{\Omega} \bar{u} \mathcal{D}_u + \bar{v} \mathcal{D}_v + \bar{w} \mathcal{D}_w dx dy + \oint_{\Gamma} \bar{u} \bar{n}_y N_{xy} - \partial_y \bar{w} \bar{n}_y M_{yy} \\ & + \bar{v} (\bar{n}_x N_{xy} + \bar{n}_y N_{yy}) + \bar{w} \bar{n}_y (\partial_y M_{yy} + 2\partial_x M_{xy} \\ & + N_{xy} \partial_x w + N_{yy} \partial_y w) ds + \int_0^b [\bar{u} (N_{xx} - \hat{N}_{xx,L})]_{x=L} \\ & + [\partial_x \bar{w} (-M_{xx})]_{x=L} dy = 0, \end{aligned}$$

where \bar{n}_x and \bar{n}_y are the directional cosines of the unit normal vector (e.g. $\bar{n}_x = 0$ and $\bar{n}_y = -1$ at the edge $y = 0$), and \bar{u} , \bar{v} , and \bar{w} are weighting functions. After partial integration, the weak form can be expressed as

$$\begin{aligned} & \int_{\Omega} \bar{u} \rho h (V^2 \partial_x^2 u + g) + \bar{v} \rho h V^2 \partial_x^2 v + \bar{w} \rho h (V^2 \partial_x^2 w \\ & + 2V \partial_x \partial_t w + \partial_t^2 w) + \partial_x \bar{u} N_{xx} + \partial_y \bar{u} N_{xy} + \partial_y \bar{v} N_{yy} \\ & + \partial_x \bar{v} N_{xy} - \partial_x^2 \bar{w} M_{xx} - 2\partial_{xy}^2 \bar{w} M_{xy} - \partial_y^2 \bar{w} M_{yy} \\ & + \partial_x \bar{w} (N_{xx} \partial_x w + N_{xy} \partial_y w) + \partial_y \bar{w} (N_{xy} \partial_x w + N_{yy} \partial_y w) \\ & - \bar{w} q dx dy = \int_0^b \bar{u}|_{x=L} \hat{N}_{xx,L} dy. \end{aligned} \quad (10)$$

For spatial discretization, the strip is divided into n rectangular finite elements along the direction x as indicated in Fig. 1. They have the element number $e \in \{1, 2, \dots, n\}$ and arbitrary length $a_e = x_{e,\max} - x_{e,\min}$. The strip displacements are approximated by the trial functions

$$u = \sum_{e=1}^n \sum_{i=0}^{n_x} \sum_{j=0}^{n_{yu}} X_{e,i}(x) Y_j(y) T_{e,ij}^u(t) \quad (11a)$$

$$v = \sum_{e=1}^n \sum_{i=0}^{n_x} \sum_{j=0}^{n_{yv}} X_{e,i}(x) Y_j(y) T_{e,ij}^v(t) \quad (11b)$$

$$w = \sum_{e=1}^n \sum_{i=0}^{n_x} \sum_{j=0}^{n_{yw}} X_{e,i}(x) Y_j(y) T_{e,ij}^w(t), \quad (11c)$$

with four basis functions ($n_x = 3$) in longitudinal direction and freely selectable numbers of basis functions in lateral direction (according to n_{yu} , n_{yv} , and n_{yw}). The time functions $T_{e,ij}^u(t)$, $T_{e,ij}^v(t)$, and $T_{e,ij}^w(t)$ are the Galerkin coefficients. $X_{e,i}(x)$ and $Y_j(y)$ are defined as

$$X_{e,i}(x) = \begin{cases} \bar{X}_{e,i}(x - x_{e,\min}) & \text{if } x_{e,\min} \leq x \leq x_{e,\max} \\ 0 & \text{else} \end{cases}$$

$$Y_j(y) = \sum_{s=0}^{Z_j} \frac{(-1)^s (2j - 2s)! \left(\frac{2y}{b} - 1\right)^{j-2s}}{2^j s! (j - s)! (j - 2s)!},$$

with

$$\begin{aligned} \bar{X}_{e,0}(\bar{x}) &= 2\bar{x}^3/a_e^3 - 3\bar{x}^2/a_e^2 + 1 \\ \bar{X}_{e,1}(\bar{x}) &= -\bar{x}^3/a_e^2 + 2\bar{x}^2/a_e - \bar{x} \\ \bar{X}_{e,2}(\bar{x}) &= -2\bar{x}^3/a_e^3 + 3\bar{x}^2/a_e^2 \\ \bar{X}_{e,3}(\bar{x}) &= -\bar{x}^3/a_e^2 + \bar{x}^2/a_e, \end{aligned}$$

where

$$Z_j = \frac{j}{2} - \frac{1}{4} \left(1 - (-1)^j\right).$$

The trial functions $\bar{X}_{e,i}(\bar{x})$ are Hermite polynomials and $Y_j(y)$ are Legendre polynomials. Products of the type $X_{e,i}(x) Y_j(y)$ are used as weighting functions \bar{u} , \bar{v} , and \bar{w} . Using Hermite polynomials as trial functions has particularly advantages, if a geometrical boundary condition is independent of the y -coordinate. This is the case for boundary condition B, where the deflection \hat{u}_L is equal to the coefficient of the product $X_{n,2} Y_0$. The number of DOF of the resulting problem can be reduced by $n_{yu} + 1$. In a similar manner, the boundary conditions $\hat{w}_{x,0}$ and \hat{w}_0 can be realized. The matrix-vector representation of the dynamical system obtained after substitution of the weighting and trial functions into (10) can be written as

$$(V^2 \mathbf{H}^{uv} + \mathbf{K}^{uv}) \mathbf{T}^{uv} = \mathbf{F}^{uv}(t) - \mathbf{h}(\mathbf{T}) \quad (12a)$$

$$\mathbf{M}^w \ddot{\mathbf{T}} + 2V \mathbf{G}^w \dot{\mathbf{T}} + [V^2 \mathbf{H}^w + \mathbf{K}^w(\mathbf{T}^{uv}, \mathbf{T})] \mathbf{T} = \mathbf{F}^w(t). \quad (12b)$$

Here, the vectors \mathbf{T} and \mathbf{T}^{uv} are arranged in the form

$$\mathbf{T} = [(\mathbf{T}_{1,2})^T, \dots, \underbrace{(\mathbf{T}_{e-1,e})^T, (\mathbf{T}_{e,e+1})^T}_{(\mathbf{T}_e)^T}, \dots, (\mathbf{T}_{n,n+1})^T]^T$$

$$\mathbf{T}^{uv} = [(\mathbf{T}^u)^T, (\mathbf{T}^v)^T]^T,$$

where \mathbf{T}^u and \mathbf{T}^v have a similar but not identical structure compared to \mathbf{T} . The sub-vectors

$$\begin{aligned} \mathbf{T}_e^u &= [T_{e,00}^u, T_{e,01}^u, \dots, T_{e,0n_{yu}}^u, T_{e,10}^u, \dots, T_{e,n_x n_{yu}}^u]^T \\ \mathbf{T}_e^v &= [T_{e,00}^v, T_{e,01}^v, \dots, T_{e,0n_{yv}}^v, T_{e,10}^v, \dots, T_{e,n_x n_{yv}}^v]^T \\ \mathbf{T}_e &= [T_{e,00}^w, T_{e,01}^w, \dots, T_{e,0n_{yw}}^w, T_{e,10}^w, \dots, T_{e,n_x n_{yw}}^w]^T \end{aligned}$$

correspond to the element e . In (12), time derivatives are denoted with dots as superscripts. The in-plane stiffness matrix is denoted as \mathbf{K}^{uv} . The matrix $\mathbf{K}^w(\mathbf{T}^{uv}, \mathbf{T})$ accounts for the stiffness in transverse direction and depends on the in-plane displacements (membrane stress), on the out-of-plane displacements (bending stress), and on residual stresses in the strip. The matrices \mathbf{H}^{uv} and \mathbf{H}^w depend on the centrifugal forces, $2V \mathbf{G}^w$ constitutes the Coriolis force and \mathbf{M}^w is the mass matrix for the out-of-plane motion. Effects due to the gravity force, a constant displacement \hat{u}_L or in-plane loads like the tensile load $\hat{N}_{xx,L}$, and the in-plane residual strain parameters $\epsilon_{xx,res}^0$, $\epsilon_{yy,res}^0$ and $\gamma_{xy,res}^0$ are included in the vector $\mathbf{F}^{uv}(t)$. Transversal loads q , residual stresses in the strip, and contributions due to non-zero values of the boundary conditions ($x = 0$) are taken into account in $\mathbf{F}^w(t)$. As a consequence of the geometrically nonlinear theory, the vector $\mathbf{h}(\mathbf{T})$ describes the nexus between in-plane and transversal displacements.

3.2 Time Integration

Solving (12a) for \mathbf{T}^{uv} and insertion into (12b) yields the residuum

$$\mathbf{r} = \mathbf{M}^w \ddot{\mathbf{T}} + 2V \mathbf{G}^w \dot{\mathbf{T}} + [V^2 \mathbf{H}^w + \bar{\mathbf{K}}^w(\mathbf{T}, t)] \mathbf{T} - \mathbf{F}^w(t) = \mathbf{0} \quad (13)$$

with the abbreviation

$$\bar{\mathbf{K}}^w(\mathbf{T}, t) = \mathbf{K}^w \left((V^2 \mathbf{H}^{uv} + \mathbf{K}^{uv})^{-1} [\mathbf{F}^{uv}(t) - \mathbf{h}(\mathbf{T})], \mathbf{T} \right).$$

The corresponding initial conditions \mathbf{T}_0 and $\dot{\mathbf{T}}_0$ can be determined from (9). \mathbf{T} can now be computed by solving the nonlinear ODE (13). For this purpose the Modified

Generalized- α Method (cf. Shearer and Cesnik, 2006) is applied, which is a tailored solver for structural dynamic problems. The idea is to predict the values and respective time derivatives of the next time step (predictor step). A subsequent correction based on the Newton-Raphson method in combination with a line search minimizes the residuum \mathbf{r} as long as a desired tolerance is achieved (corrector step). Fig. 2 outlines the time integration scheme, which is similar to the one proposed by G eradin and Rixen (1997). The first step is to initialize the procedure, e.g., the computation of the constant mass matrix \mathbf{M}^w and the definition of the initial conditions \mathbf{T}_0 and $\dot{\mathbf{T}}_0$. In the second block, the initial acceleration $\ddot{\mathbf{T}}_0$ is computed. Now all three states at the time step $m = 0$ are specified and the main procedure can be executed with the time increment (step size) $\Delta t = t_{m+1} - t_m$.

1. *Prediction:* To predict the values at the time step $m + 1$, G eradin and Rixen (1997) proposes the relations

$$\mathbf{T}_{m+1}^* = \mathbf{T}_m + \Delta t \dot{\mathbf{T}}_m + \left(\frac{1}{2} - \beta\right) \Delta t^2 \ddot{\mathbf{T}}_m \quad (14a)$$

$$\dot{\mathbf{T}}_{m+1}^* = \dot{\mathbf{T}}_m + (1 - \gamma) \Delta t \ddot{\mathbf{T}}_m \quad (14b)$$

$$\ddot{\mathbf{T}}_{m+1}^* = \mathbf{0}, \quad (14c)$$

where the superscript star refers to a prediction. The values \mathbf{T}_m , $\dot{\mathbf{T}}_m$, and $\ddot{\mathbf{T}}_m$ at the present time step m are known. Shearer and Cesnik (2006) related the parameters β and γ with the adjustment of the dissipation of high frequency modes. The parameter ρ_∞ can vary from 1 (no dissipation) to 0 (asymptotic annihilation)

$$\begin{aligned} \gamma &= \frac{1}{2} - \alpha_m + \alpha_f \\ \beta &= \frac{1}{4} (1 - \alpha_m + \alpha_f)^2 \\ \alpha_m &= \frac{2\rho_\infty - 1}{\rho_\infty + 1} \\ \alpha_f &= \frac{\rho_\infty}{\rho_\infty + 1}. \end{aligned}$$

2. *Correction:* Expansion of the residuum into a Taylor series and neglecting higher order terms yields

$$\mathbf{r}_{m+1}^{k+1} = \mathbf{r}_{m+1}^k + \mathbf{S}(\mathbf{T}_{m+1}^k) \Delta \mathbf{T}_{m+1}^k, \quad (15)$$

with the Jacobian matrix

$$\mathbf{S}(\mathbf{T}_{m+1}^k) = \left[\frac{\partial \mathbf{r}_{m+1}}{\partial \mathbf{T}} \right]_{\mathbf{T}_{m+1}^k},$$

where k denotes the iteration index. Utilizing the relations

$$\frac{\partial \ddot{\mathbf{T}}}{\partial \mathbf{T}} = \frac{1}{\beta \Delta t^2} \mathbf{I} \quad \text{and} \quad \frac{\partial \dot{\mathbf{T}}}{\partial \mathbf{T}} = \frac{\gamma}{\beta \Delta t} \mathbf{I}$$

suggested by G eradin and Rixen (1997), with the identity matrix \mathbf{I} , the Jacobian matrix can be written as

$$\begin{aligned} \mathbf{S}(\mathbf{T}) &= \mathbf{M}^w \frac{1}{\beta \Delta t^2} + 2V \mathbf{G}^w \frac{\gamma}{\beta \Delta t} \\ &+ \left[V^2 \mathbf{H}^w + \frac{\partial}{\partial \mathbf{T}} (\bar{\mathbf{K}}^w(\mathbf{T}, t)) \right]. \end{aligned}$$

The displacement correction is obtained from (15) by setting $\mathbf{r}_{m+1}^{k+1} = \mathbf{0}$

$$\Delta \mathbf{T}_{m+1}^k = - [\mathbf{S}(\mathbf{T}_{m+1}^k)]^{-1} \mathbf{r}_{m+1}^k$$

and the values and their time derivatives are corrected in the form

$$\mathbf{T}_{m+1}^{k+1} = \mathbf{T}_{m+1}^k + \Delta \mathbf{T}_{m+1}^k \quad (16a)$$

$$\dot{\mathbf{T}}_{m+1}^{k+1} = \dot{\mathbf{T}}_{m+1}^k + \frac{\gamma}{\beta \Delta t} \Delta \mathbf{T}_{m+1}^k \quad (16b)$$

$$\ddot{\mathbf{T}}_{m+1}^{k+1} = \ddot{\mathbf{T}}_{m+1}^k + \frac{1}{\beta \Delta t^2} \Delta \mathbf{T}_{m+1}^k. \quad (16c)$$

The iteration is repeated as long as a desired residuum $\|\mathbf{r}_{m+1}^{k+1}\| < r_{\min}$ is achieved. For systems with a large number of DOF, the situation $\|\mathbf{r}_{m+1}^{k+1}\| > \|\mathbf{r}_{m+1}^k\|$ may occur. Shearer and Cesnik (2006) recommended to extend the Newton-Raphson method with a line search algorithm to overcome this difficulty. The method is not further discussed in this paper. To ensure a benign numerical

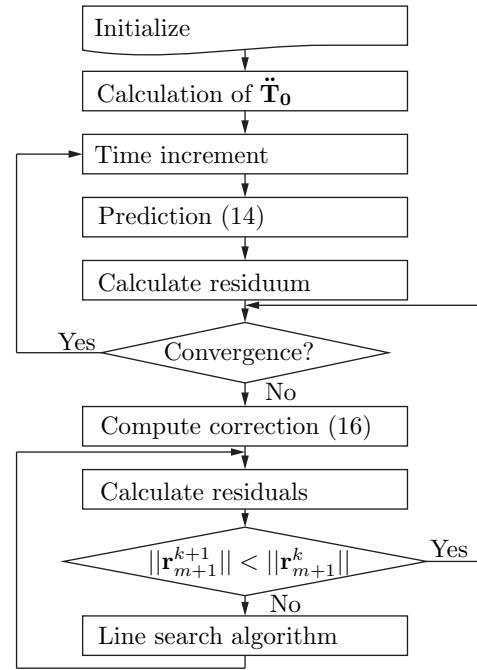


Fig. 2. Implicit time integration method.

behavior, the dimensionless parameters

$$\tilde{u} = \frac{u}{L}, \quad \tilde{v} = \frac{v}{L}, \quad \tilde{w} = \frac{w}{L}, \quad \tilde{x} = \frac{x}{L}, \quad \tilde{y} = \frac{y}{L}, \quad \tilde{b} = \frac{b}{L}, \quad \tilde{h} = \frac{h}{L}$$

$$\tilde{t} = \frac{t}{L} \sqrt{\frac{\hat{N}_{xx,L}/h}{\rho}}, \quad \tilde{V} = V \sqrt{\frac{\rho}{\hat{N}_{xx,L}/h}}, \quad \tilde{E} = \frac{E}{\hat{N}_{xx,L}/h}$$

$$\tilde{q} = \frac{q}{\hat{N}_{xx,L}/h}, \quad \tilde{N}_{xx} = \frac{N_{xx}}{\hat{N}_{xx,L}}, \quad \tilde{N}_{yy} = \frac{N_{yy}}{\hat{N}_{xx,L}}, \quad \tilde{N}_{xy} = \frac{N_{xy}}{\hat{N}_{xx,L}}$$

are used throughout all numerical simulations (cf. Shin et al., 2006).

4. HOT DIP GALVANIZING PLANT

As an example, axially moving steel strips can be found in hot dip galvanizing lines, see Fig. 3. The strip length of the plant is $L = 56.5$ m, which was discretized into 89 elements of different lengths. Elements near to the stabilization and tower rolls are chosen smaller than the inner ones.

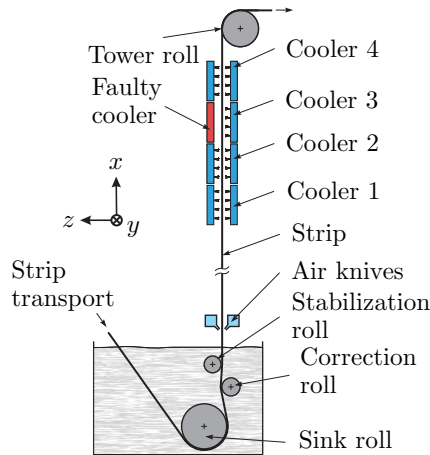


Fig. 3. A typical hot dip galvanizing line with an air cooler.

The mass density is assumed to be $\rho = 7850 \text{ kg/m}^3$. The dimensions of the coolers and their pressure loads $q = q_c$ on the strip can be found in (Saxinger et al., 2015). The number of trial functions in lateral direction are chosen as $n_{yu} = n_{yv} = 7$ and $n_{yw} = 4$. All subsequent studies are summarized in the Section 5.

4.1 Frequency Analysis

First, the influence of the initial strip displacement and boundary conditions for $\hat{N}_{xx,L}$ (boundary condition A) and \hat{u}_L (boundary condition B) on the oscillation frequency f of the strip is studied in simulations. In order to conduct this analysis, the strip defined in Table 1 without any residual stresses is assumed. Fig. 4 shows the results of this analysis for various initial shapes $\bar{w}_0 = \max|w_0|$, and $w_1 = 0$. They are determined by means of an eigenvalue analysis after linearization of the system at $w = 0$. The simulations for the nonlinear systems have been performed with the time integration procedure described in Section 3.2, where $\rho_\infty = 0.99$ was used. For a prescribed tensile load $\hat{N}_{xx,L}$ (boundary condition A), the frequencies of the strip vibrations are virtually identical with the frequencies determined by means of the eigenvalue analysis. This behavior is independent of \bar{w}_0 and the shape of the strip. Different characteristics can be observed for a prescribed displacement \hat{u}_L (boundary condition B): the frequencies of the strip vibrations increase for larger values of \bar{w}_0 , and they strongly depend on the shape of the strip.

Table 1. Strip data without residual stresses.

$\frac{b}{\text{m}}$	$\frac{h}{\text{mm}}$	$\frac{\hat{w}_0}{\text{mm}}$	$\frac{\hat{w}_{x,0}}{\text{m/m}}$	$\frac{\hat{N}_{xx,L}}{\text{kN/m}}$	$\frac{E}{\text{N/m}^2}$	$\frac{V}{\text{m/s}}$
1.48	0.95	0	0	31.1	$1.58 \cdot 10^{11}$	0

4.2 Stationary Shape of the Strip if a Cooler Fails

In the next simulation, the displacement \hat{w}_0 and the slope $\hat{w}_{x,0}$ are prescribed at the stabilization roll. The residual strain parameters and the boundary conditions at the stabilization roll are computed according to Baumgart et al. (2015). In this paper, an elasto-plastic beam model for the strip shape in the zinc pot and the associated residual stresses are presented. The dimensions and boundary

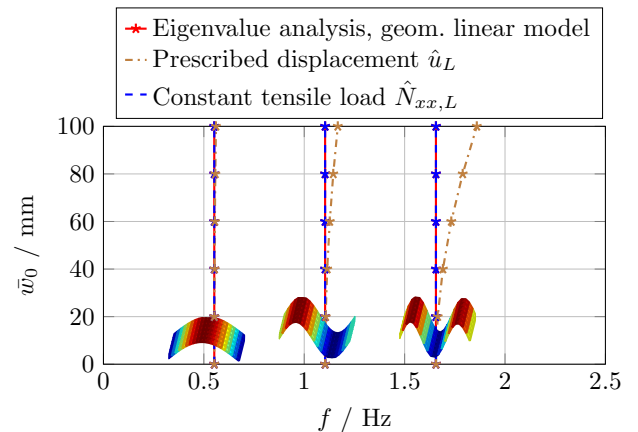


Fig. 4. Frequency of strip vibrations for different initial displacements \bar{w}_0 and boundary conditions.

conditions of three different strips are listed in Table 2. Table 3 contains the non-zero quantities of the residual strain parameters of these strips determined on the basis of the elasto-plastic beam model. The quantities $\gamma_{xy,res}^0$ and $\gamma_{xy,res}^1$ are set to zero for all strips and the strip velocity is $V = 105 \text{ m/min}$.

Table 2. Dimensions and boundary conditions.

Strip	$\frac{b}{\text{m}}$	$\frac{h}{\text{mm}}$	$\frac{\hat{w}_0}{\text{mm}}$	$\frac{\hat{w}_{x,0}}{\text{m/m}}$	$\frac{\hat{N}_{xx,L}}{\text{kN/m}}$
A	1.34	0.5	0.074	-0.034	24.2
B	1.66	1.5	0.063	-0.032	27.7
C	1.48	0.95	0.22	-0.06	31.1

Table 3. Residual strain parameters.

Strip	$\frac{E}{\text{N/m}^2}$	$\frac{\epsilon_{xx,res}^0}{10^{-3}}$	$\frac{\epsilon_{yy,res}^0}{10^{-3}}$	$\frac{\epsilon_{xx,res}^1}{1/\text{m}}$	$\frac{\epsilon_{yy,res}^1}{1/\text{m}}$
A	$1.6 \cdot 10^{11}$	0.5402	-0.0629	-0.3856	0.2415
B	$1.56 \cdot 10^{11}$	0.0611	-0.0081	-0.1752	-0.0118
C	$1.58 \cdot 10^{11}$	0.3592	-0.0274	-0.4110	0.2629

In the following, the impact of a faulty cooler on the steady-state strip shape is investigated. In this scenario, which is indicated in Fig. 3, one half of cooler 3 does not supply cooling air (zero pressure load). All other coolers operate at the same pressure level p , which is varied in the simulations below. The maximum transverse displacement w_{max} of the geometrically nonlinear model as well as the maximum transverse error $e_{max} = \max|w_N - w_L|$ between the geometrically linear (subscript L) and nonlinear (subscript N) models for a prescribed tensile load $\hat{N}_{xx,L}$ can be seen in Fig. 5. Corresponding results for a prescribed displacement \hat{u}_L are shown in Fig. 6. As a consequence of the residual stresses in the strip, a small error can be observed even for $p = 0$. A higher pressure level p causes a higher transverse displacement w . The increased pressure p leads to a rise in the error for both simulations. However, the error is approximately 10 times higher, if the boundary condition is a prescribed displacement \hat{u}_L (boundary condition B). Fig. 7 shows the steady-state shape of the strip A for $p = 25 \text{ mbar}$ and $\hat{N}_{xx,L} = 24.2 \text{ kN/m}$ computed by the geometrically nonlinear model.

5. CONCLUSIONS

The main findings of this work are as follows:

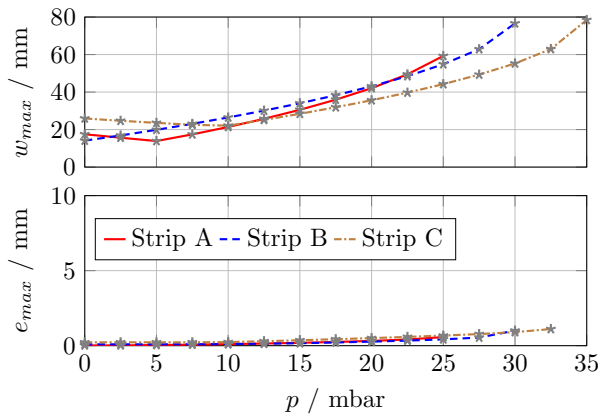


Fig. 5. Maximum displacement of geometrically nonlinear model and deviation of linear model for a prescribed tensile load $\hat{N}_{xx,L}$.

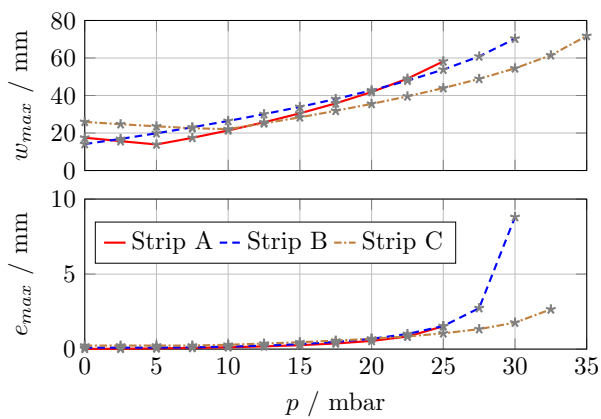


Fig. 6. Maximum displacement of geometrically nonlinear model and deviation of linear model for a prescribed displacement \hat{u}_L .

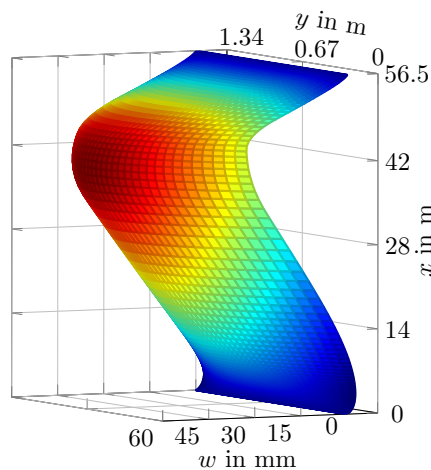


Fig. 7. Steady-state shape of strip A for $p = 25$ mbar and $\hat{N}_{xx,L} = 24.2$ kN/m (geometrically nonlinear model).

- Depending on the boundary condition at the tower roll, e.g., a prescribed tensile load $\hat{N}_{xx,L}$ or a prescribed displacement \hat{u}_L , different deviations between

geometrically nonlinear and linear models can be observed.

- The geometrically linear model with a tensile load $\hat{N}_{xx,L}$ boundary condition is sufficiently accurate for most applications.
- When larger displacements are expected for a strip with a prescribed displacement \hat{u}_L boundary condition, the geometrically nonlinear model should be used.
- There is only an insignificant difference in the oscillation frequencies between the geometrically linear and nonlinear model for the a prescribed tensile load $\hat{N}_{xx,L}$.
- Larger initial transverse strip displacements w_0 lead to higher vibrational frequencies for a prescribed displacement \hat{u}_L . The frequencies are strongly influenced by the shape of the strip.

REFERENCES

- Baumgart, M., Steinböck, A., Saxinger, M., and Kugi, A. (2015). Elasto-plastic bending of steel strip in a hot-dip galvanizing line. In *Proceedings of the 3rd Polish Congress of Mechanics (PCM) and 21st International Conference on Computer Methods in Mechanics (CMM)*, 55–56. Gdansk, Poland.
- Chung, J. and Hulbert, G.M. (1993). A time integration algorithm for structural dynamics with improved numerical dissipation: The generalized-alpha method. *Journal of Applied Mechanics*, 60, 371–375.
- Géradin, M. and Rixen, D. (1997). *Mechanical Vibrations: Theory and Application to Structural Dynamics*. Wiley, Chichester, 2nd edition.
- Hira, T., Abe, H., and Azuma, S. (1988). Analysis of sheet metal bending deformation behavior in processing lines and its effectiveness. (19), 54–62.
- McIver, D. (1973). Hamilton’s principle for systems of changing mass. *Journal of Engineering Mathematics*, 7(3), 249–261.
- Reddy, J. (2007). *Theory and Analysis of Elastic Plates and Shells*. CRC Press, Boca Raton, London, New York, 2nd edition.
- Saxinger, M., Steinböck, A., Baumgart, M., Kerschbaummayr, P., and Kugi, A. (2015). Influence of air cooling jets on the steady-state shape of strips in hot dip galvanizing lines. In *Proceedings of the 4th IFAC Workshop on Mining, Mineral and Metal Processing (MMM)*, volume 48, 143–148. Oulu, Finland.
- Shearer, C. and Cesnik, C. (2006). Modified generalized α method for integrating governing equations of very flexible aircraft. In *Proceedings of the 47th AIAA/ASME/ASCE/AHS/ASC Structures, Structural Dynamics, and Materials Conference*. Newport, Rhode Island, USA.
- Shin, C., Chung, J., and Hee Yoo, H. (2006). Dynamic responses of the in-plane and out-of-plane vibrations for an axially moving membrane. *Journal of Sound and Vibration*, 297(3–5), 794–809.
- Steinboeck, A., Baumgart, M., Stadler, G., Saxinger, M., and Kugi, A. (2015). Dynamical models of axially moving rods with tensile and bending stiffness. In *Proceedings of the 8th Vienna International Conference on Mathematical Modelling (MATHMOD)*, 598–603. Vienna, Austria.